DOI: 10.1002/eji.202048556 Eur. J. Immunol. 2020. 50: 1976–1987

Basic

European Journal of Immunology

Immunity to infection

Research Article

Intestinal microbiota disruption limits the isoniazid mediated clearance of *Mycobacterium tuberculosis* in mice

Shikha Negi[1,2], *Susanta Pahari*[1,3], *Hilal Bashir*[1] *and Javed N. Agrewala*[1,4]

[1] Immunology Division, CSIR-Institute of Microbial Technology, Chandigarh, India
[2] Present address: Department of Medicine, Washington University in St. Louis, St. Louis, Missouri, USA
[3] Immunology Division, Texas Biomedical Research Institute, San Antonio, Texas, USA
[4] Centre for Biomedical Engineering, Indian Institute of Technology-Ropar, Rupnagar, Punjab, India

Tuberculosis (TB) continues to remain a global threat due to the emergence of drug-resistant *Mycobacterium tuberculosis* (*Mtb*) strains and toxicity associated with TB drugs. Intestinal microbiota has been reported to affect the host response to immunotherapy and drugs. However, how it affects the potency of first-line TB drug isoniazid (INH) is largely unknown. Here, we examined the impact of gut microbial dysbiosis on INH efficiency to kill *Mtb*. In this study, we employed in vivo mouse model, pretreated with broad-spectrum antibiotics (Abx) cocktail to disrupt their intestinal microbial population prior to *Mtb* infection and subsequent INH therapy. We demonstrated that microbiota disruption results in the impairment of INH-mediated *Mtb* clearance, and aggravated TB-associated tissue pathology. Further, it suppressed the innate immunity and reduced CD4 T-cell response against *Mtb*. Interestingly, a distinct shift of gut microbial profile was noted with abundance of *Enterococcus* and reduction of *Lactobacillus* and *Bifidobacterium* population. Our results show that the intestinal microbiota is crucial determinant in efficacy of INH to kill *Mtb* and impacts the host immune response against infection. This work provides an intriguing insight into the potential links between host gut microbiota and potency of INH.

Keywords: antibiotics · innate immunity · intestinal microbiota · isoniazid · tuberculosis · T cells

Additional supporting information may be found online in the Supporting Information section at the end of the article.

Introduction

Mycobacterium tuberculosis (*Mtb*) is one of the successful pathogens that causes the disease tuberculosis (TB). *Mtb* affects millions of people worldwide and surmounted HIV in terms of mortality and morbidity [1, 2]. It is estimated that only 10-15%

Correspondence: Prof. Javed N. Agrewala
e-mail: jagrewala@iitrpr.ac.in

of the *Mtb* infected individuals, develop active TB, while remaining has the potential of *Mtb* reactivation later in their lifetime [3]. Emergence of drug-resistant strains of *Mtb*, HIV pandemic, variable BCG efficacy, lengthy Directly Observed Treatment Short-course (DOTS) regime, and TB drugs-associated side effects are among the factors that impede the successful treatment of the disease [4, 5]. Since 1950s, isoniazid also known as isonicotinyl hydrazide (INH) is one of the effective front-line drugs to treat TB [6]. Further, drug therapy often renders patients to suffer from refractory TB [7]. This suggests that even the currently available TB drugs fail to completely eradicate *Mtb* and, thus, imparts inadequate protection to the host. Rather in few patients, TB drugs, including INH have been reported to induce side effects such as hepatotoxicity and suppressed host immunity [8, 9].

Apart from the INH mediated targeting of mycolic acids synthesis in *Mtb*, few reports suggest the interaction between INH and host immune system. INH treatments have been shown to decline the IFN-γ level in TB patients [10]. In addition, T-cells apoptosis induced by INH is found to be responsible for reinfection and reactivation of *Mtb* [11]. TB drugs also hamper the cathelicidin (antimicrobial peptide) level, which is required for the inhibition of *Mtb* growth by targeting autolysosomal process [12]. Further, it was reported that during *Mtb* infection, bacteria induced IL-1R, and TNF-α cytokines affect INH-mediated *Mtb* clearance [13]. These evidences suggest the interplay of INH and host factors that may affect the drug efficacy to treat TB.

Dysbiosis of the intestinal commensal population is known to trigger and aggravate several disorders such as cancer, allergy, autoimmune diseases, and infections [14–18]. Interestingly, commensals have been reported to modulate the efficacy of anti-cancer drugs and antibody-based therapies [19]. For instance, the efficacy of checkpoint inhibitor, PD-L1 was augmented by the commensal *Bifidobacterium* in a tumour mice model. This was caused by enhancing the function of DCs, resulting in the effective antitumor CD8 T-cell response [20]. Moreover, depletion of microbiota impaired the response of tumour-surrounding myeloid-derived cells to platinum chemotherapy and CpG-oligonucleotide immunotherapy. This was accompanied by the poor cytokine production and ROS generation in these mice [21]. These studies highlight the role of intestinal microbiota in the success and failure of therapies in host. In addition, microbiota boost *Escherichia coli* clearance in the lungs of mice through TLR4 activation [22]. Notably, *Mtb* infection leads to the significant gut microbial changes in mice [23]. Further, high-fat diet induced gut dysbiosis was also found to be responsible for TB disease progression [24].

Antibiotics (Abx) often prescribed for treating various ailments have been shown to alter the gut microbiota composition [25, 26]. Recently, we have demonstrated that disturbances in gut microbiota resulted in increased susceptibility to *Mtb* infection in mice [27, 28]. Further, TB drug therapy has been shown to modulate the host intestinal microbial community profile and immunity [18, 29–31]. Here, we hypothesized that disruption of gut microbiota compromises the efficacy of INH therapy to kill *Mtb*. Consequently, our study shows that Abx impaired the INH efficiency to restrict *Mtb* survival in the experimental model of TB.

Results

Gut microbiota regulates intestinal integrity and immunity during INH therapy in *Mtb* infected mice

To address the importance of intestinal microbiota during INH therapy, mice were subjected to the combination of broad-spectrum Abx (vancomycin, neomycin, and metronidazole) to disrupt the microbial population (Supporting information Fig. S1A and B) prior to the starting of INH therapy in *Mtb* challenged mice. The experimental design for this study is shown in Fig. 1A.

Microbiota disruption resulted in the enlargement of caecum in Abx treated versus CT ($p < 0.05$), Abx-*Mtb* versus *Mtb* infected ($p < 0.01$), and Abx-*Mtb*-INH versus *Mtb*-INH ($p < 0.01$) mice. This indicates accumulation of food which is normally digested by bacteria and decreases contraction ability of intestine [32] (Fig. 1B and C). Further, the histopathological examination showed distorted intestinal epithelium architecture and discontinuity of epithelial barrier in Abx, Abx-*Mtb*, and Abx-*Mtb*-INH group (Fig. 1D).

The production of defense peptide, such as RegIII-γ (Regenerating islet-derived lectins), is regulated by beneficial commensals and affects innate immunity in the intestine [33, 34]. *RegIII* γ gene expression declined in the Abx-*Mtb* and Abx-*Mtb*-INH mice relative to *Mtb* and *Mtb*-INH group, respectively (Fig. 1E). Furthermore, contrary to the upregulation of anti-inflammatory *Il 10*, these mice exhibited downregulation of proinflammatory cytokines, *Tnf* α, and *Ifn* γ in their intestine (Fig. 1F-H).

Abx induce profound gut microbiota changes in mice during INH therapy in *Mtb* infected mice

Any perturbations in the gut microbial composition can affect the host immunity to infections [35]. Thus, we next investigated the gut microbial profile in fecal DNA samples of mice by qRT-PCR. As compared to *Mtb* challenged group, mice treated with Abx showed decrease in the total intestinal bacteria load. Further, decline was noticed in the Abx-*Mtb*-INH group relative to the *Mtb*-INH mice, indicating loss of total gut bacteria (Fig. 2A). At genus level, Abx-*Mtb*-INH mice relative to *Mtb*-INH, exhibited significant reduction of *Lactobacillus* ($p < 0.01$), *Bifidobacterium* ($p < 0.001$), and *Campylobacter* ($p < 0.05$) population (Fig. 2B-D). On the contrary, *Bacteroides* ($p < 0.01$) and *Enterococcus* ($p < 0.01$) population was increased in these mice (Fig. 2E and F). Similar loss of bacterial genus, such as *Lactobacillus*, *Bifidobacterium,* and *Campylobacter*, was observed in the Abx-*Mtb* versus *Mtb* and Abx versus control (CT) mice.

Disruption of intestinal microbiota limits the INH-mediated *Mtb* clearance

Abx treatment showed increase in the *Mtb* burden of ~0.5 log in lungs relative to the *Mtb* infected mice. Animals with INH therapy

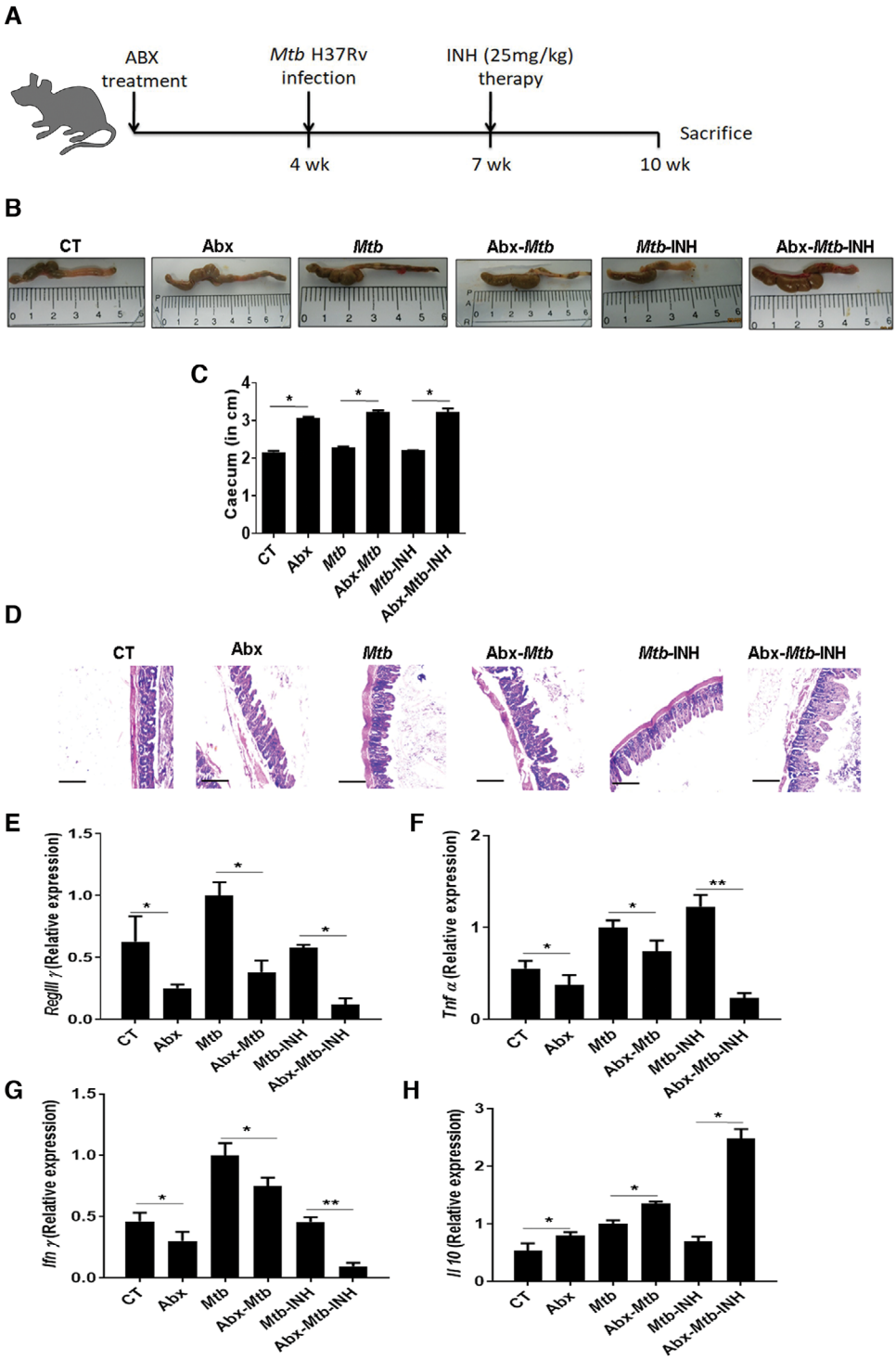

Figure 1. Microbiota disruption during INH therapy affects the intestinal barrier and immunity. (A) Mice were given *ad libitum* access to the broad-spectrum Abx cocktail consisting of vancomycin (500 mg/L), neomycin (1 g/L), and metronidazole (1 g/L) in drinking water for 4 weeks prior to *Mtb* infection (~100 CFU of H37Rv). After the establishment of infection (21 days post-infection), INH (25 mg/kg of body weight) therapy was provided by oral route for 3 weeks (5 days/wk) to the infected mice. Later, (B, C) size of caecum was measured; bar graph shows the caecum length in cm; (D) haematoxylin and eosin stained histopathological sections of small intestine showing ileal structures (scale bar, 50 μm and 100X); (E-H) mRNA transcript levels of (E) *RegIII γ*; (F) *Tnf α;* (G) *Ifn γ;* and (H) *Il10* in small intestine was quantified by qRT-PCR. Fold change was calculated with reference to β-actin as control. Data expressed as mean ± SEM are representative of two to three independent experiments (n = 4–5 mice/group). Parametric *t*- test was used after Shapiro–Wilk normality test for statistical analysis. $^{*}p < 0.05$, $^{**}p < 0.01$. CT: control mice; Abx: mice treated with Abx alone; *Mtb*: *Mtb* challenged mice; Abx-*Mtb*: mice treated with Abx prior to *Mtb* infection; *Mtb*-INH: mice challenged with *Mtb* followed by INH therapy; Abx-*Mtb*-INH: Abx-treated mice infected with *Mtb* prior to INH therapy.

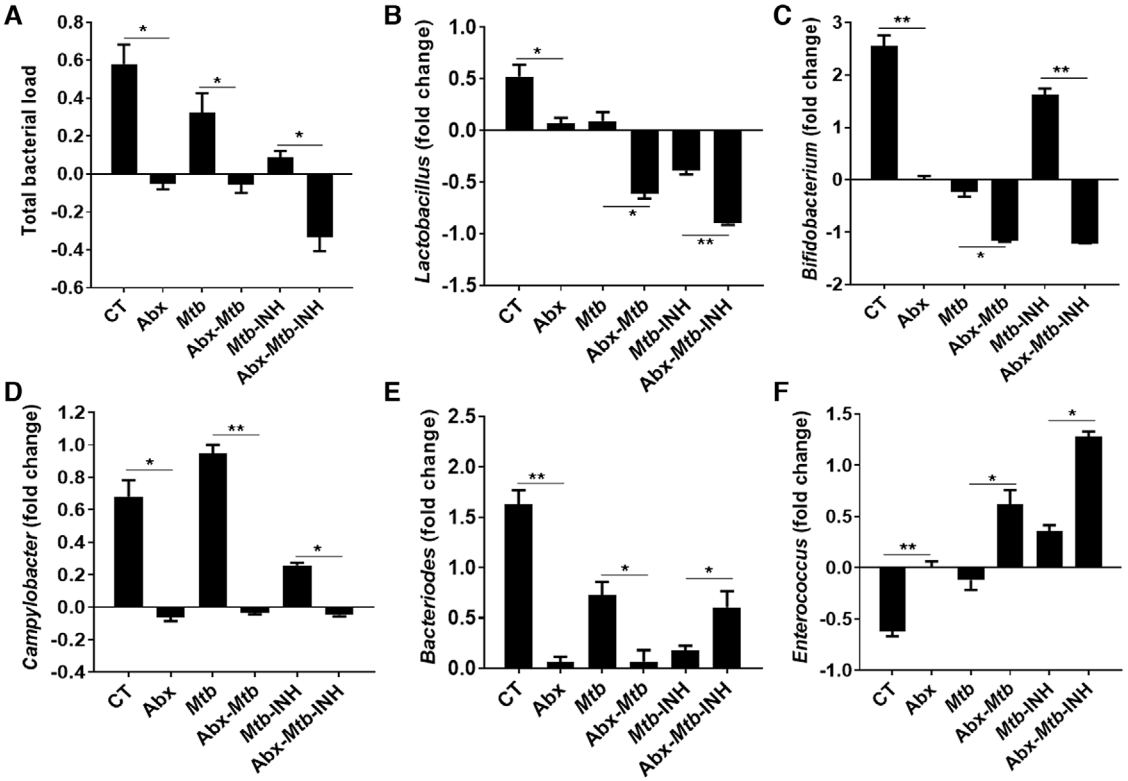

Figure 2. Abx treatment alters gut microbial profile in mice undergoing INH therapy. Mice were treated with Abx cocktail, followed by *Mtb* infection and INH administration as described in the legend to Fig. 1A. Later, DNA was isolated from fecal samples of mice for quantitative PCR analysis and normalized to universal bacterial primer. Bar graphs depict (A) total bacterial load; (B-F) bacterial genus such as (B) *Lactobacillus*; (C) *Bifidobacterium*; (D) *Campylobacter*; (E) *Bacteroides*; and (F) *Enterococcus*. Bacterial abundance was depicted as fold change relative to Abx group and normalized to universal bacterial primer. The effect of Abx-alone was subtracted, and comparative analysis was done with Abx group. Data represented as mean ± SEM are of three independent experiments (n = 4–5 mice/group). Parametric *t*-test was used after Shapiro–Wilk normality test for statistical analysis. $^{*}p < 0.05$, $^{**}p < 0.01$.

(*Mtb*-INH) exhibited significant reduction of *Mtb* CFU, compared to the *Mtb*-INH ($p < 0.001$) and Abx-*Mtb* ($p < 0.01$) group. However, microbiota disruption resulted in the reduction of INH-mediated *Mtb* clearance as illustrated by increased ($p < 0.01$) CFUs in the lungs of Abx-*Mtb*-INH mice versus *Mtb*-INH group. Thus, the difference in *Mtb* versus *Mtb*-Abx and *Mtb*-INH versus Abx-*Mtb*-INH group is approximately five- and 15-fold, respectively (Fig. 3A). Further, histopathological analysis of lung tissue substantiated the CFU results. INH treated (*Mtb*-INH) versus *Mtb* infected group exhibited small and less granulomatous regions. In contrast, Abx-*Mtb* and Abx-*Mtb*-INH mice displayed high number of granulomas with more consolidated confluent areas and infiltration of lymphocytes (Fig. 3B and C).

Gut microbiota disruption during INH therapy abrogates *Mtb* specific T-cell response in mice

Effector and memory T cells are essential to restrict the *Mtb* growth [36, 37]. To determine the status of CD4 T cells, we assessed the expression of CD44 and CD62L in lung cells. Upon *Mtb* infection, proportion of activated CD4 T cells ($CD44^{hi}$) was increased, as compared to CT group. However, upon Abx treatment, there was a substantial decline in the pool of $CD44^{hi}$ CD4 T cells. Notably, INH therapy in *Mtb* infected mice (*Mtb*-INH) also reduced the activated CD4 T-cell population. Abx-mediated microbiota disruption in Abx-*Mtb*-INH group further depleted the $CD44^{hi}$ CD4 T-cell population in lungs (Fig. 4A and B). Moreover, the percentage of central and effector memory ($CD62L^{lo}CD44^{hi}$) CD4 T cells were also found to be reduced in these mice (Fig. 4C and D). Unlike INH, Abx did not seem to affect the proliferation of CD4 T cells. As the CD4 T cells of *Mtb*-INH and Abx-*Mtb*-INH mice proliferated poorly in response to *Mtb* purified protein derivative antigen (PPD) (Fig. 4E and F).

Interestingly, INH therapy has been implicated in the apoptosis of activated CD4 T cells [11]. However, gut dysbiosis did not affect the Annexin V positive population in mouse lungs (Supporting information Fig. S3).

Intestinal microbiota disruption during INH therapy abolishes innate immune response against *Mtb*

Innate immune response is detrimental to restrict *Mtb* at an early stage of infection and elicit activation of adaptive immunity [38]. $CD11c^{+}$ $CD11b^{+}$ myeloid cells, such as DCs, are the specialized cells of innate immunity that regulates T-cells activation and differentiation [39]. Interestingly, we observed that upon gut

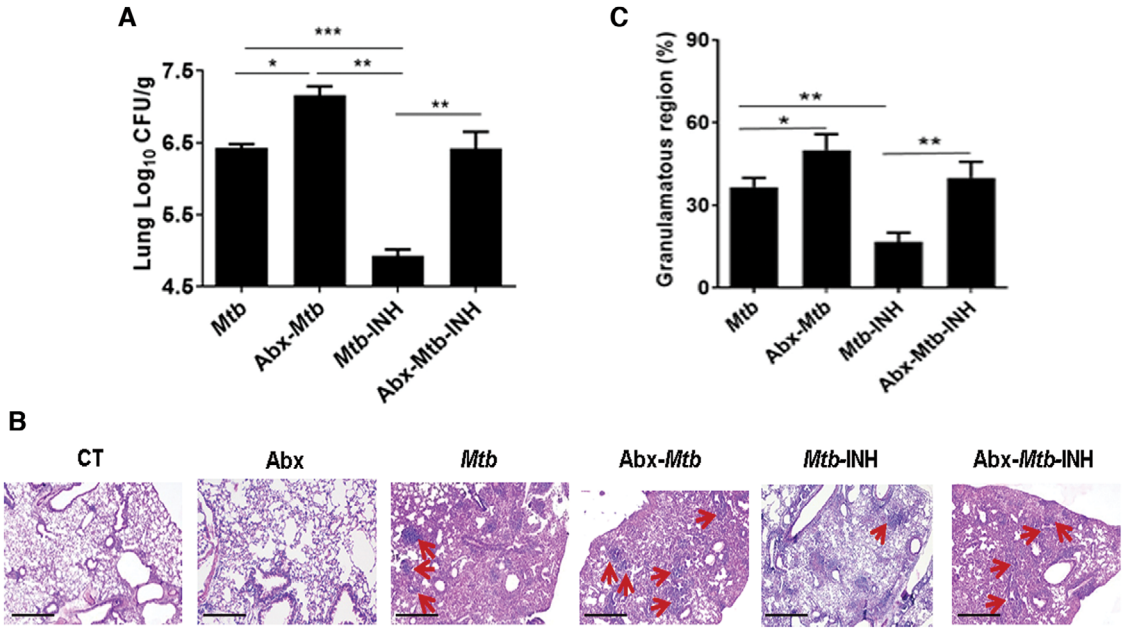

Figure 3. Intestinal microbiota disruption impedes INH-mediated *Mtb* clearance. Mice were given Abx cocktail for 4 weeks prior to *Mtb* infection. After 21 days, INH therapy was initiated for subsequent 3 weeks. Thereafter, lung tissue was assessed for (A) bacillary load by CFU assay. Bar diagrams represent the *Mtb* load; (B) histopathological changes by H&E staining, images examined at 40X magnification and scale bar, 50 μm; (C) bar graph represents the percentage of granulomatous region. Arrows indicate granulomas in the lung specimen. Data expressed as mean ± SEM are of three independent experiments, n = 4–5 mice/group. One-way ANOVA followed by Tukey multiple comparison test after Shapiro–Wilk normality test was used for statistical analysis of the groups. $^{*}p < 0.05$, $^{**}p < 0.01$, $^{***}p < 0.001$.

microbiota disruption, lung myeloid DCs ($CD11c^{+}$ $CD11b^{+}$) in Abx-*Mtb* versus *Mtb* exhibited downregulation in the expression of MHC-II and CD86. In comparison to *Mtb* group, animals with INH therapy (*Mtb*-INH) showed reduction in MHC-II and CD86 levels. This was further dampened by Abx as seen in Abx-*Mtb*-INH group and consequently reflects the diminished antigen presentation ability and activation of myeloid DCs in lungs (Fig. 5A and B). Additionally, we observed low levels of IFN-γ and TNF-α cytokines in their lung cell culture supernatants (Fig. 5C and D).

Abx downregulates the proinflammatory cytokines production in Abx-*Mtb* mice versus *Mtb* group. Further, the lungs of Abx-*Mtb*-INH mice relative to *Mtb*-INH, showed significantly lower expression of *Il 1β* ($p < 0.01$), *Il 6* ($p < 0.01$), and *Il 12* ($p < 0.05$). Conversely, level of anti-inflammatory cytokine *Il 10*, which is known for downregulating protective anti-TB response was found to be significantly ($p < 0.001$) higher as demonstrated through qRT-PCR analysis (Fig. 6A-D). Moreover, in comparison to *Mtb*-INH mice, microbiota disruption reduced the expression of innate receptors, such as *Tlr 2* ($p < 0.05$), *Mincle* ($p < 0.05$), and *Nod 2* ($p < 0.01$), in Abx-*Mtb*-INH group (Fig. 6E-G). These data confirm that intestinal microbiota disruption during INH therapy further impairs the innate immune response of host against *Mtb*.

Discussion

In this study, we aimed to assess our hypothesis of whether Abx intake as a prophylactic measure or their misuse may compromise the efficacy of isoniazid (INH) and immune response against *Mtb* infection. INH is a frontline drug used for treating TB. It restricts the *Mtb* survival by targeting the synthesis of mycolic acids, which is a vital component of the *Mtb* cell wall [1]. However, the influence of intestinal microbiota on INH efficacy to restrict *Mtb* survival has not been well studied.

The role of intestinal microbiota has been extensively recognized in modulating the host immunity during homeostasis and infections [15, 40–42]. Recently, our laboratory reported the enhanced susceptibility to *Mtb* upon ablation of gut microbiota [28]. Further, intestinal bacteria have been shown to influence the host response to antitumor therapies [21, 43]. Previous reports suggest that anti-TB drugs can induce significant gut microbiota changes and compromises immunity [18, 29, 30]. But the effect of intestinal microbiota disruption on INH potency to kill *Mtb* remains unexplored. Using in vivo murine model of TB, we observed diminished intestinal immunity in microbiota disrupted animals that were undergoing INH therapy as the level of *RegIII γ* [33] (antimicrobial peptide) declined. Moreover, proinflammatory cytokines, such as TNF-α and IFN-γ, which play an important role in host immune response were found to be decreased [44]. However, gut dysbiosis elevated the levels of anti-inflammatory cytokine, IL-10 in these animals. These findings suggest that disturbances in gut microbiota during INH therapy can impair the intestinal innate defense and immunity.

INH therapy led to dramatic changes in gut microbial composition as seen by the abundance of *Bifidobacterium* and *Enterococcus* and decrease in *Bacteroides*, *Campylobacter*, and *Lactobacillus* genus. Interestingly, Abx-induced dysbiosis during INH therapy shifted this gut microbial profile as there was reduced prevalence

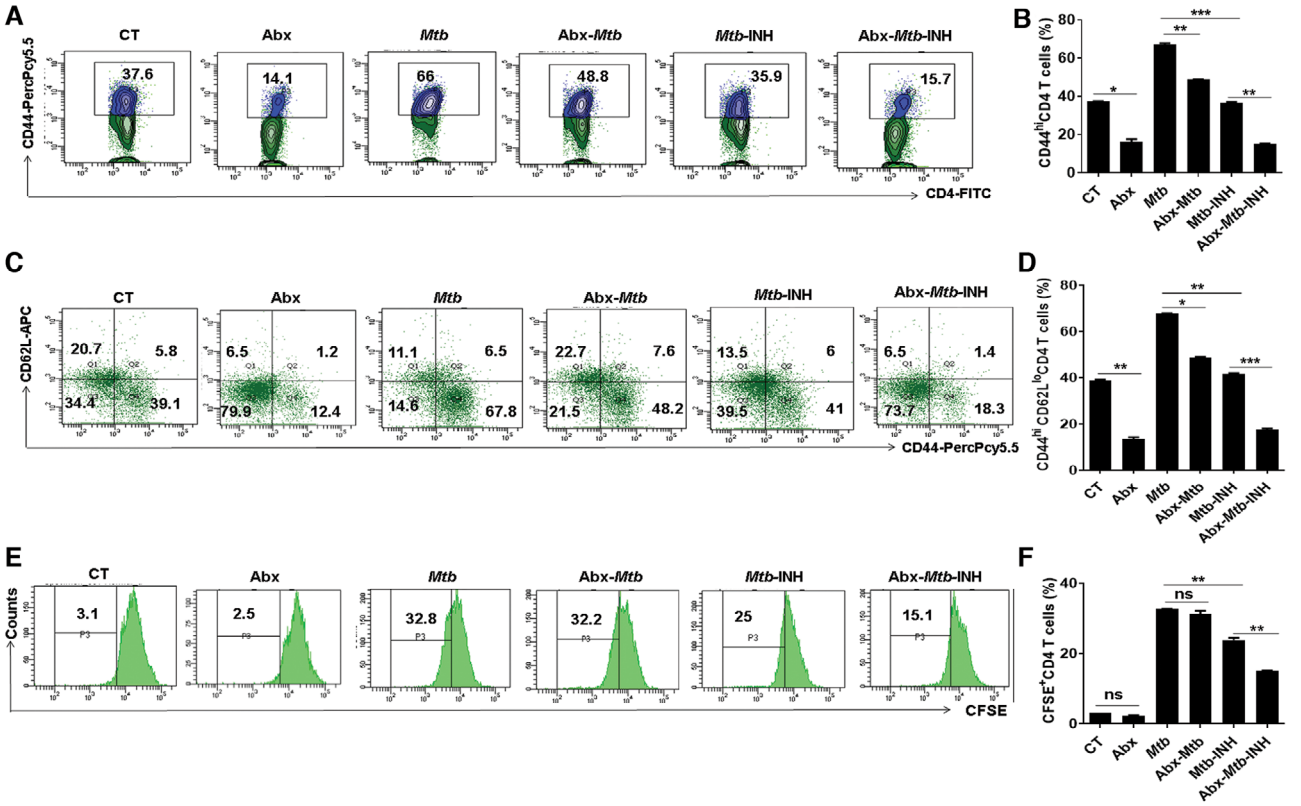

Figure 4. Gut dysbiosis reduces CD4 T-cell memory pool during INH therapy. Microbiota-disrupted mice were aerosol infected with *Mtb* and then subjected to INH therapy as indicated in legend to Fig. 1A. Later, animals were sacrificed, and lung cells were isolated. (A-D) Thereafter, cells were stained with anti-CD3, CD4, CD44, CD62L antibodies, and assessed for the (A,B) expression of $CD44^{hi}$ population representing activated CD4 T cells; (C,D) CD44 and CD62L population for effector ($CD44^{hi}$ $CD62L^{lo}$) and central ($CD44^{hi}$ $CD62L^{lo}$) memory CD4 T cells; (E,F) lung cells were labeled with CFSE (2 μM) and cultured in the presence of PPD (25 μg/mL) for 72 h then evaluated for CD4 T-cells proliferation. The flow cytometry plots (dot plots/contour plots/histograms) and bar diagram indicate the percent population gated on $CD3^+$ CD4 T cells. Data expressed as mean ± SEM, n = 4–5 mice/group and representative of two to three independent experiments. One-way ANOVA followed by Tukey multiple comparison test after Shapiro–Wilk normality test was used for statistical analysis of the groups. ns: nonsignificant, $^*p < 0.05$, $^{**}p < 0.01$, $^{***}p < 0.001$.

of commensals, such as *Bifidobacterium*, *Campylobacter*, and *Lactobacillus*, while *Enterococcus* and *Bacteroides* population were found to be highly abundant. Notably, *Lactobacillus* and *Bifidobacterium* are known for their beneficial immunomodulatory properties [45–47]. These findings suggest the contribution of intestinal bacteria in determining the host immune response to INH treatment. It is possible that microbiota disruption resulted in a decreased population of beneficial commensals that impaired the immune response to INH therapy in efficiently restricting the *Mtb* survival. This observation is supported by the increased *Mtb* burden and development of more severe granulomatous regions in the lungs.

CD4 T cells play an inevitable role in protection against *Mtb* [36]. Our results indicate that gut dysbiosis in INH-treated mice resulted in impairment of T-cell activation, proliferation, and memory T-cells generation. Consequently, the host immunity could not adequately contribute in restricting the *Mtb* growth.

Previously, it has been reported that gut microbiota affects host response to cancer therapies by modulating tumor-infiltrating myeloid cells [19, 20]. Myeloid cells, such as DCs, are the key cells to mount innate immune response and activates T cells during *Mtb* infection [39, 48, 49]. This process requires efficient expression of MHC-II and costimulatory molecules such as CD86. Consistent with the attenuated T-cell response, intestinal microbiota disruption during INH therapy, led to the impairment of lung myeloid DCs ($CD11c^+$ $CD11b^+$), as observed by downregulation in the expression of MHC-II and CD86 along with decline in the yield of IFN-γ and TNF-α cytokines that are involved in restricting *Mtb* growth [50, 51]. Further, cytokines, such as IL-1β (elicits NO production), IL-12 (induce Th1 response), and IL-6, are required for the protective immune response against *Mtb* [52–54]. Gut dysbiosis in mice during INH therapy significantly decreased the transcripts level of these cytokines. Additionally, the immune recognition of *Mtb* components by pattern recognition receptors (PRRs) plays a crucial role in the immune cells activation and production of protective proinflammatory cytokines [54–59]. The observed cytokines profile and $CD11c^+$ $CD11b^+$ cells phenotype were consistent with the defect in innate immune sensing as PRRs, such as NOD-2, TLR-2, and Mincle were observed to be decreased on the decimation of gut microbiota in INH administered mice. However, the exact mechanism of interaction between specific innate cells and gut microbiota; second, the direct effect of intestinal microbes in regulating immune response during INH therapy remains to be addressed. Further, the lack of comprehensive characterization and evaluation of microbiome changes upon dysbiosis during INH

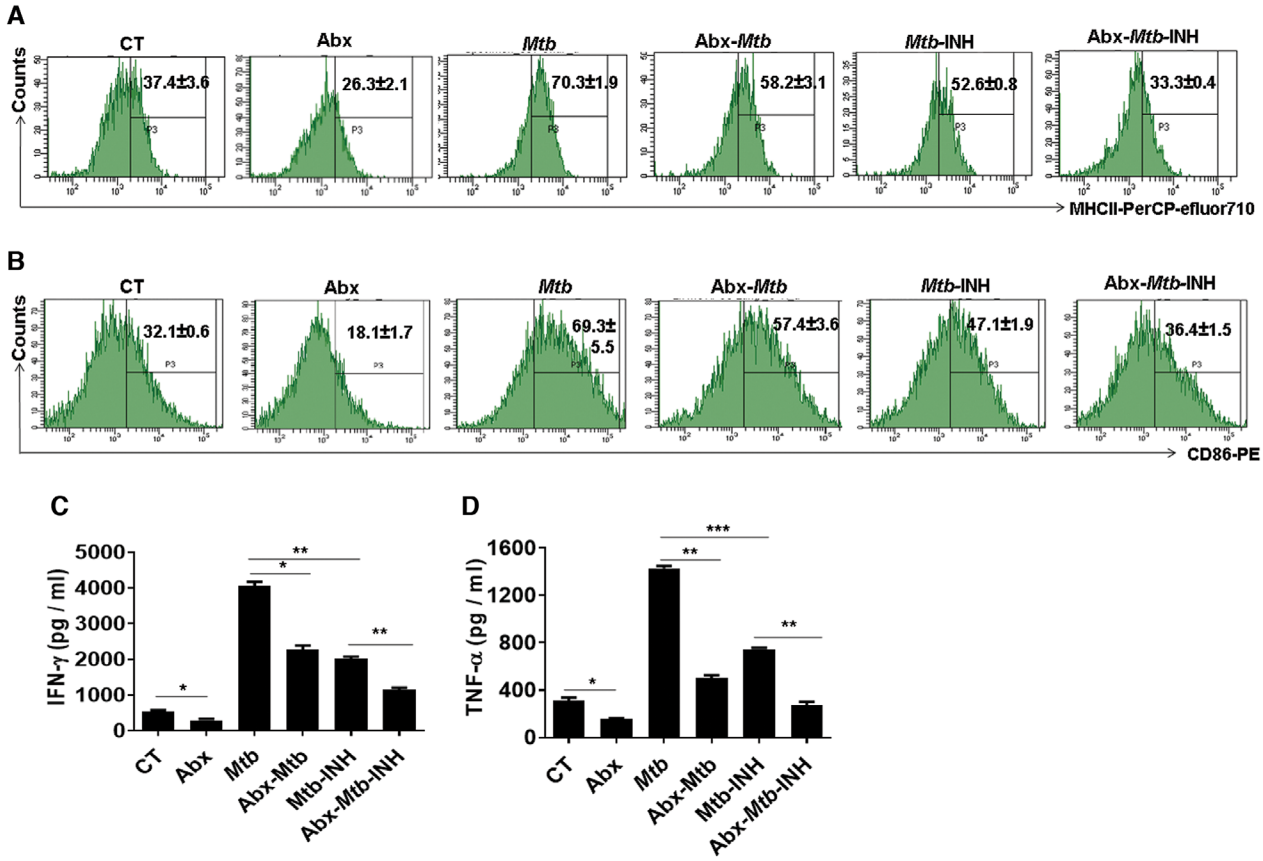

Figure 5. Downregulation of MHC-II and CD86 in myeloid DCs and impaired release of IFN-γ and TNF-α in lungs of microbiota disrupted mice during INH therapy. Commensals disrupted mice were infected with *Mtb* prior to INH therapy. Later, mice were sacrificed, and lung tissue was harvested, and (A-B) cells were stained to assess (A) MHC-II; (B) CD86 expression through flow cytometry, histograms indicate the percentage of cells gated on $CD11c^+$ $CD11b^+$ myeloid DC population. (C-D) Lung cells were cultured in the presence of PPD (25 μg/mL) for 48 h, followed by estimation of (C) IFN-γ; and (D) TNF-α levels in cell culture SNs by ELISA. Data represented as mean ± SEM and representative of two independent experiments (n = 4–5 mice/group). One-way ANOVA followed by Tukey multiple comparison test after Shapiro–Wilk normality test was performed. $^*p < 0.05$, $^{**}p < 0.01$, $^{***}p < 0.001$.

therapy is another limitation of the study, which suggests the future line of investigation. This study depicts that Abx-induced intestinal dysbiosis compromised the host innate and adaptive immune response, eventually affecting the *Mtb* restricting potency of INH. In future, a better understanding of gut microbes and their impact on host response to TB drugs can pave ways for developing new and effective TB therapies. Development of probiotics using beneficial gut microbes and their combinatorial therapy with drugs may improve the efficiency of TB drugs to treat the disease and improve host immunity against *Mtb*.

Materials and methods

Study design

A brief overview of the experimental strategy used in the study is shown in Fig. 1A. To investigate the effects of intestinal microbiota on INH efficacy, mice were divided into five groups namely, CT: control mice (untreated and uninfected); Abx: mice treated with Abx alone; *Mtb*: *Mtb* challenged mice; Abx-*Mtb*: mice treated with Abx prior to *Mtb* infection; *Mtb*-INH: mice challenged with *Mtb* followed by INH therapy; Abx-*Mtb*-INH: Abx-treated mice infected with *Mtb* prior to INH therapy ($n = 5$ mice per group). The CT, *Mtb*, and *Mtb*-INH groups were given water, while the other groups were on Abx till the end of experiment. For the antibiotic treatment, mice were given a cocktail of broad-spectrum Abx (Sigma) containing vancomycin (0.5 g/L), neomycin sulfate (1 g/L), and metronidazole (1 g/L) *ad libitum* in drinking water for 4 weeks (via a water bottle) prior to the *Mtb* infection and INH therapy. To assess the load of cultivable microbes upon Abx treatment, stool samples were plated on BHI medium in aerobic and anaerobic conditions for 48 h at 37ºC. Each experiment was repeated at least two times.

Mice and ethical statement

Female C57BL/6 mice of age 6-7 weeks (20 ± 2 g body weight) were obtained from the Animal Facility of the CSIR-Institute of Microbial Technology (IMTECH), Chandigarh, India. The animals were reared under conventional conditions (in a

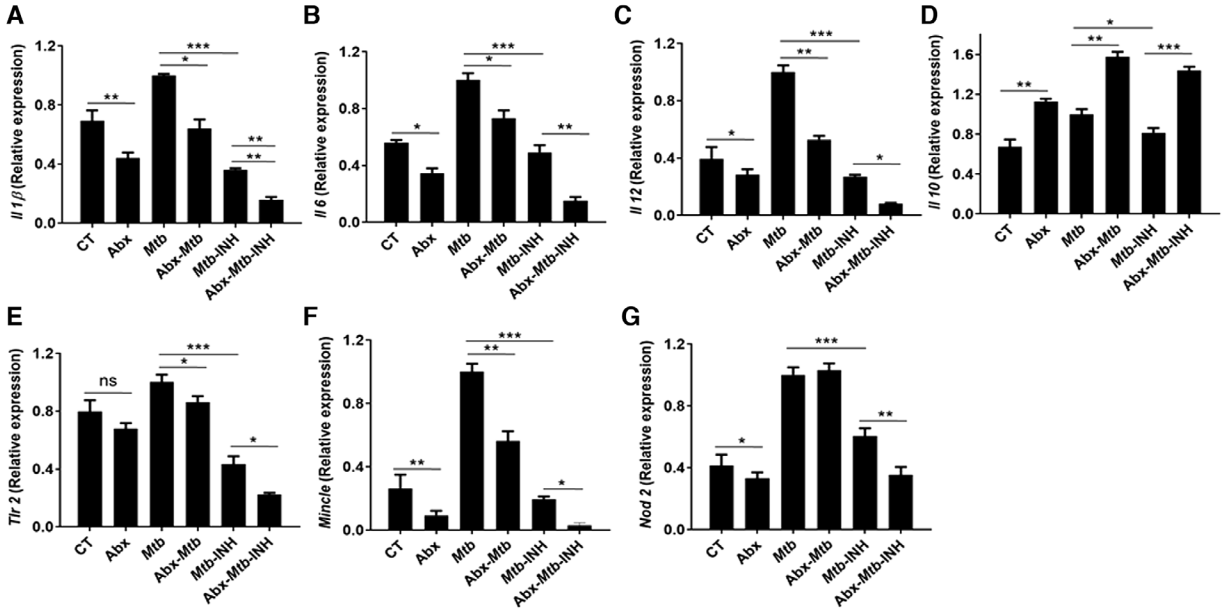

Figure 6. Expression levels of cytokines and innate receptors in lungs of microbiota disrupted mice during INH therapy. Microbiota disrupted mice were infected with *Mtb* prior to INH therapy as described in the legend to Fig. 1A. Later, mice were sacrificed, and lung tissue was harvested and evaluated for the gene expression of (A) *Il 1β*; (B) *Il 6*; (C) *Il 12*; (D) *Il 10*; (E) *Tlr 2*; (F) *Mincle*; and (G) *Nod 2* through qRT-PCR analysis. Bar graphs represent fold change with β-actin as control. Data shown as mean ± SEM are of two to three independent experiments, n = 4–5 mice/group. ns: nonsignificant, $^{*}p < 0.05$, $^{**}p < 0.01$, $^{***}p < 0.001$. One-way ANOVA followed by Tukey multiple comparison test after Shapiro–Wilk normality test was performed.

temperature-controlled room (25 ± 2°C) under a 12 h light/dark cycle at IMTECH Animal facility.

All the mice experiments and protocols in the study were approved by the Institutional Animal Ethics Committee (IAEC) of CSIR-IMTECH and experiments were accomplished in accordance with the National Regulatory Guideline issued by Committee for the Purpose of Control and Supervision of Experiments on Animals (No. 55/1999/CPCSEA), Ministry of Environment and Forest, Government of India.

Reagents

All the reagents were obtained from Sigma Aldrich (St. Louis, MO, USA), unless otherwise mentioned. Fluorochrome-conjugated antibodies: CD4-FITC, CD44-PercPcy5.5, CD62L-APC, CD86-PE, and MHCII-PerCP-efluor710, CD11c-PEcy7, CD11b-APC-Cy7, CD8-PEcy7, CD3-APC-Cy7, CD64-FITC, Annexin V-FITC, ELISA reagents, and antibodies were procured from BD Pharmingen (San Diego, CA, USA). L-glutamine, streptomycin, L-pyruvate, and penicillin were brought from Serva (Heidelberg, Germany). The fetal bovine serum (FBS) was obtained from GIBCO (Grand Island, NY, USA). All tissue culture grade plastic ware was bought from BD Biosciences (San Diego, CA, USA).

Mtb aerosol infection, INH drug therapy, and CFU assay

Mtb strain H37Rv was grown in Middlebrook 7H9 broth with albumin (10%), dextrose, catalase, and Tween-80 (0.05%), and glycerol (0.2%). Later, 20% glycerol stocks of H37Rv were made and stored at −80°C for infection experiments. Mice were infected with H37Rv (~100 CFU/mouse) using aerosol machine Inhalation Exposure System (Glas-Col, Terre Haute, IN, USA). After 21 days, INH (25 mg/kg of body weight) therapy was given to mice by oral gavage for 3 weeks (5 days per wk). Animals were maintained in BSL-3 laboratory. Later, animals were sacrificed, lungs were harvested, homogenized in PBS, and plated onto 7H11 agar plates supplemented with 10% OADC (Difco™, Detroit, MI, USA) followed by incubation at 37°C for 3 weeks. Thereafter, colonies were counted to calculate CFUs per gram of tissue.

Quantitative real-time PCR (qRT-PCR)

Total RNA was extracted from the small intestine and lung tissues using trizol reagent, according to the manufacturer's protocol (Invitrogen, Carisbad, CA, USA). Briefly, RNA was isolated and quantified by NanoDrop spectrophotometer (BioTek, Winooski, VT, USA). A260/A280 ratio of RNA samples was in the range of 1.9 to 2 and was, thus, considered as pure. The contaminated DNA was further removed by incubating sample with amplification grade DNase1 enzyme. RNA samples (2 μg) were incubated with DNase 1 (3 U) at RT for 15 min in reaction buffer. Later, DNase activity was terminated by adding stop solution and incubation at 72°C for 10 min. The cDNA was prepared with maxima cDNA synthesis kit. The real-time PCR analysis was done on Applied Biosystems step one plus PCR (Waltham, MA, USA) by comparative *Ct* method. The *Ct* values were normalized to house-keeping control

gene actin. The change in the gene expression was depicted as fold change. Primers used in the qRT-PCR are listed in Supporting information Table 1.

Fecal sample collection and DNA extraction

Fecal samples were collected aseptically and immediately placed on ice and stored at −80°C. Fecal DNA was isolated from 150 mg of feces using Zymo Research Fecal DNA isolation Kit (Irvine, CA, USA), as per the manufacturer's instructions. Briefly, fecal samples were homogenized with lysis buffer followed by DNA binding to the column and later, eluted in nuclease-free water. DNA was further quantified using a NanoDrop spectrophotometer (BioTek). DNA was used for real-time PCR analysis.

Bacterial genus-specific quantitative PCR

For gut bacteria quantification, extracted genomic DNA (50-100 ng), primers (0.2 μM), and SYBR green PCR Mastermix (Applied Biosystems, San Diego, CA, USA) were used for the real-time PCR reaction. Real-time PCR reactions were performed in a step one plus PCR (Applied Biosystems, Waltham). The temperature profile for the qPCR amplification was 10 min at 95°C, followed by 40 cycles of 30 s at 95°C, 1 min at 60°C. Specific genus abundance was expressed as fold change. The values were normalized to the universal bacteria DNA/primer (internal control). The 16S gene copies (total bacterial load) in the fecal samples were expressed as $\log_{10}$ copy number per gram of feces and samples were run along with known concentration of plasmid DNA as standards [60, 61]. The primers used for gut microbial analysis are listed in Supporting information Table S2 [62–65].

Lymphocytes culture

Mice were sacrificed and perfused with cold PBS containing EDTA. Thereafter, lungs were removed, and the single-cell suspension was prepared. RBCs were removed using ACK lysis buffer (GIBCO, Gaithersburg, MD, USA). The cells were resuspended in complete media (RPMI 1640 + 10% FCS) and cultured with purified protein derivative (PPD, 25 μg/mL) at a density of 2.5×10^5 cells/well in 96-well U-bottom plates at 37°C, 5% CO_2. For myeloid DCs prior to PPD stimulation, lung cells were incubated overnight in plastic tissue culture plate to eliminate adherent macrophage population.

Flow cytometric analysis

The cells were surface stained with fluorochrome tagged antibodies to evaluate the activation status of lymphoid and myeloid cells, and memory phenotype according to the guidelines [66]. Briefly, cells were incubated with Fc block for 30 min/4ºC. After washing, cells were stained with fluorochrome-conjugated antibodies against CD3, CD4, CD8, CD44, CD62L, CD11c, CD11b, CD64, MHC II, and CD86 and their respective isotype-matched control antibodies. Regular incubation and washings were done at each step. Finally, cells were fixed in paraformaldehyde (1%). The flow cytometry data were acquired using FACS ARIA-II (BD Biosciences) and analyzed by BD FACS DIVA and FlowJo software (San Jose, CA, USA). The gating strategy used for T-cells markers and myeloid DC analysis is shown in Supporting information Figs. S2 and S4, respectively.

Proliferation of T cells

The cells (2×10^5/well) were incubated with CFSE dye (2 μM) for 8 min at RT, washed to remove unbound dye, and were incubated overnight at 37°C/5% CO_2 in the culture medium. After 72 h, cells were counterstained with PB conjugated anti-CD4 antibody for 30 min at RT. Later, cells were washed (with PBS + 2% FBS) and fixed with 1% formaldehyde and further assessed through flow cytometry.

Annexin V staining to assess apoptosis

The cells were incubated with FITC conjugated Annexin V (5 μL/tube/10^6 cells) at a dilution of 1:20 in binding buffer (HEPES: 0.1 M, NaCl: 1.4 M, $CaCl_2$: 25 mM in water). The cells were incubated in dark for 15 min at RT. After washing, cells were resuspended in 1% binding buffer. Then, the cells were immediately acquired (FACS ARIA-II) and analysis was performed employing BD FACS DIVA software (San Jose, CA, USA).

Estimation of cytokines by ELISA

The cytokines, such as IFN-γ and TNF-α, were quantified in the cell culture supernatants (SNs) by standard sandwich ELISA method. In brief, 96-well ELISA plates were coated overnight with anti-TNF-α (2 μg/mL) and IFN-γ (2 μg/mL) primary antibodies in phosphate buffer (pH 9.2, 0.1M) at 4°C. The unbound sites were blocked with 1% BSA for 2-3 h at RT. Later, respective recombinant cytokines were used as standard and supernatants (50 μL) were added to the wells followed by incubation for 16 h at 4°C. Later, biotinylated anti-mouse TNF-α (2 μg/mL) and IFN-γ (2 μg/mL) antibodies were diluted (in PBS-Tween buffer) and added to the plates followed by incubation for 2 h at RT. Further, avidin-HRP (1:10 000 dilutions) was added and incubated at 37°C for 45 min. The color reaction was developed by OPD + H_2O_2 (chromogen-substrate). The reaction was stopped by H_2SO_4 (7%). The absorbance of color was read at 492 nm. The data represented as pg/mL of released cytokines were calculated using the standard curve drawn with standards of rTNF-α and rIFN-γ.

Histopathology

Mice lung and intestinal tissues were fixed in buffered formalin (10%) and blocks were prepared in paraffin. The lung and

intestinal sections were stained with H&E dyes. The microscopic images were taken on the Olympus IX71 microscope (Olympus, Tokyo, Japan). The images are depicted at 40× and 100× magnifications.

Statistics

The data were subjected to the normality test using Shapiro–Wilk test prior to all statistical tests. The p value was found to be above 0.05 indicating distribution is normal. Specific statistical analyses are mentioned in the figure legends. Overall, parametric t-test and one-way ANOVA was used for pairwise and more than two groups comparison, respectively, using Prism software (V4.03, GraphPad Software, Inc. San Diego, CA, USA). In all cases, $p < 0.05$ value was considered significant.

Acknowledgments: We are thankful to Dr. BN Dutta for histopathological data analysis. This work is dedicated to our recently departed friend and colleague Mushtaq K.
The funding for the research work is granted by the Council of Scientific and Industrial Research (CSIR) and Department of Biotechnology (DBT), Ministry of Science and Technology, India (DBT grant GAP 103). SN is recipient of the DBT-fellowship and HB and SP of CSIR fellowship.

Author contributions: JNA and SN conceived the idea and designed work. SN, SP, and HB performed the experiments. Analysis, data interpretation, and manuscript writing were done by JNA and SN.

Conflict of interest: All authors declared that they have no commercial or financial conflict of interest.

References

1 **Ahmad, Z., Klinkenberg, L. G., Pinn, M. L., Fraig, M. M., Peloquin, C. A., Bishai, W. R., Nuermberger, E. L.** et al., Biphasic kill curve of isoniazid reveals the presence of drug-tolerant, not drug-resistant, *Mycobacterium tuberculosis* in the guinea pig. *J. Infect. Dis.* 2009. **200**: 1136–1143.

2 WHO, Global Tuberculosis Report 2018. WHO Organization, Geneva 2018, pp 1–277. https://doi.org/WHO/HTM/TB/2018.20

3 **Alene, K. A., Clements, A. C. A., McBryde, E. S., Jaramillo, E., Lonnroth, K., Shaweno, D. and Viney, K.**, Sequelae of multidrug-resistant tuberculosis: protocol for a systematic review and meta-analysis. *BMJ Open* 2018. **8**: e019593.

4 **Gandhi, N. R., Nunn, P., Dheda, K., Schaaf, H. S., Zignol, M., van Soolingen, D., Jensen, P.** et al., Multidrug-resistant and extensively drug-resistant tuberculosis: a threat to global control of tuberculosis. *Lancet* 2010. **375**: 1830–1843.

5 **Cox, H. S., Morrow, M. and Deutschmann, P. W.**, Long term efficacy of DOTS regimens for tuberculosis: systematic review. *BMJ* 2008. **336**: 484–487.

6 **Pierattelli, R., Banci, L., Eady, N. A., Bodiguel, J., Jones, J. N., Moody, P. C., Raven, E. L.** et al., Enzyme-catalyzed mechanism of isoniazid activation in class I and class III peroxidases. *J. Biol. Chem.* 2004. **279**: 39000–39009.

7 **van Rie, A., Warren, R., Richardson, M., Victor, T. C., Gie, R. P., Enarson, D. A., Beyers, N.** et al., Exogenous reinfection as a cause of recurrent tuberculosis after curative treatment. *N. Engl. J. Med.* 1999. **341**: 1174–1179.

8 **Woo, J., Chan, C. H., Walubo, A. and Chan, K. K.**, Hydrazine—a possible cause of isoniazid-induced hepatic necrosis. *J. Med.* 1992. **23**: 51–59.

9 **Nelson, S. D., Mitchell, J. R., Timbrell, J. A., Snodgrass, W. R. and Corcoran, G. B., 3rd**, Isoniazid and iproniazid: activation of metabolites to toxic intermediates in man and rat. *Science* 1976. **193**: 901–903.

10 **Biraro, I. A., Egesa, M., Kimuda, S., Smith, S. G., Toulza, F., Levin, J., Joloba, M.** et al., Effect of isoniazid preventive therapy on immune responses to *Mycobacterium tuberculosis*: an open label randomised, controlled, exploratory study. *BMC Infect. Dis.* 2015. **15**: 438.

11 **Tousif, S., Singh, D. K., Ahmad, S., Moodley, P., Bhattacharyya, M., Van Kaer, L. and Das, G.**, Isoniazid induces apoptosis of activated $CD4^+$ T cells: implications for post-therapy tuberculosis reactivation and reinfection. *J. Biol. Chem.* 2014. **289**: 30190–30195.

12 **Chesdachai, S., Zughaier, S. M., Hao, L., Kempker, R. R., Blumberg, H. M., Ziegler, T. R. and Tangpricha, V.**, The effects of first-line anti-tuberculosis drugs on the actions of vitamin D in human macrophages. *J. Clin. Transl. Endocrinol.* 2016. **6**: 23–29.

13 **Yamashiro, L. H., Eto, C., Soncini, M., Horewicz, V., Garcia, M., Schlindwein, A. D., Grisard, E. C.** et al., Isoniazid-induced control of *Mycobacterium tuberculosis* by primary human cells requires interleukin-1 receptor and tumor necrosis factor. *Eur. J. Immunol.* 2016. **46**: 1936–1947.

14 **Zhan, Y., Chen, P. J., Sadler, W. D., Wang, F., Poe, S., Nunez, G., Eaton, K. A.** et al., Gut microbiota protects against gastrointestinal tumorigenesis caused by epithelial injury. *Cancer Res.* 2013. **73**: 7199–7210.

15 **Kamada, N., Seo, S. U., Chen, G. Y. and Nunez, G.**, Role of the gut microbiota in immunity and inflammatory disease. *Nat. Rev. Immunol.* 2013. **13**: 321–335.

16 **Yurkovetskiy, L. A., Pickard, J. M. and Chervonsky, A. V.**, Microbiota and autoimmunity: exploring new avenues. *Cell Host Microbe* 2015. **17**: 548–552.

17 **Dumas, A., Corral, D., Colom, A., Levillain, F., Peixoto, A., Hudrisier, D., Poquet, Y.** et al., The host microbiota contributes to early protection against lung colonization by *Mycobacterium tuberculosis*. *Front. Immunol.* 2018. **9**: 2656.

18 **Khan, N., Mendonca, L., Dhariwal, A., Fontes, G., Menzies, D., Xia, J., Divangahi, M.** et al., Intestinal dysbiosis compromises alveolar macrophage immunity to *Mycobacterium tuberculosis*. *Mucosal Immunol.* 2019. **12**: 772–783.

19 **West, N. R. and Powrie, F.**, Immunotherapy not working? check your microbiota. *Cancer Cell* 2015. **28**: 687–689.

20 **Sivan, A., Corrales, L., Hubert, N., Williams, J. B., Aquino-Michaels, K., Earley, Z. M., Benyamin, F. W.** et al., Commensal *Bifidobacterium* promotes antitumor immunity and facilitates anti-PD-L1 efficacy. *Science* 2015. **350**: 1084–1089.

21 **Iida, N., Dzutsev, A., Stewart, C. A., Smith, L., Bouladoux, N., Weingarten, R. A., Molina, D. A.** et al., Commensal bacteria control cancer response to therapy by modulating the tumor microenvironment. *Science* 2013. **342**: 967–970.

22 **Tsay, T. B., Yang, M. C., Chen, P. H., Hsu, C. M. and Chen, L. W.**, Gut flora enhance bacterial clearance in lung through toll-like receptors 4. *J. Biomed. Sci.* 2011. **18**: 68.

23 **Winglee, K., Eloe-Fadrosh, E., Gupta, S., Guo, H., Fraser, C. and Bishai, W.**, Aerosol *Mycobacterium tuberculosis* infection causes rapid loss of diversity in gut microbiota. *PLoS One* 2014. **9**: e97048.

24 **Arias, L., Goig, G. A., Cardona, P., Torres-Puente, M., Diaz, J., Rosales, Y., Garcia, E.** et al., Influence of gut microbiota on progression to tuberculosis generated by high fat diet-induced obesity in C3HeB/FeJ mice. *Front. Immunol.* 2019. **10**: 2464.

25 **Hill, D. A., Hoffmann, C., Abt, M. C., Du, Y., Kobuley, D., Kirn, T. J., Bushman, F. D.** et al., Metagenomic analyses reveal antibiotic-induced temporal and spatial changes in intestinal microbiota with associated alterations in immune cell homeostasis. *Mucosal Immunol.* 2010. **3**: 148–158.

26 **Dudek-Wicher, R. K., Junka, A. and Bartoszewicz, M.**, The influence of antibiotics and dietary components on gut microbiota. *Prz Gastroenterol.* 2018. **13**: 85–92.

27 **Negi, S., Pahari, S., Bashir, H. and Agrewala, J. N.**, Gut microbiota regulates mincle mediated activation of lung dendritic cells to protect against *Mycobacterium tuberculosis*. *Front Immunol.* 2019. **10**: 1142.

28 **Khan, N., Vidyarthi, A., Nadeem, S., Negi, S., Nair, G. and Agrewala, J. N.**, Alteration in the gut microbiota provokes susceptibility to tuberculosis. *Front. Immunol.* 2016. **7**: 529.

29 **Namasivayam, S., Maiga, M., Yuan, W., Thovarai, V., Costa, D. L., Mittereder, L. R., Wipperman, M. F.** et al., Longitudinal profiling reveals a persistent intestinal dysbiosis triggered by conventional anti-tuberculosis therapy. *Microbiome* 2017. **5**: 71.

30 **Wipperman, M. F., Fitzgerald, D. W., Juste, M. A. J., Taur, Y., Namasivayam, S., Sher, A., Bean, J. M.** et al., Antibiotic treatment for Tuberculosis induces a profound dysbiosis of the microbiome that persists long after therapy is completed. *Sci. Rep.* 2017. **7**: 10767.

31 **Dubourg, G., Lagier, J. C., Armougom, F., Robert, C., Hamad, I., Brouqui, P. and Raoult, D.**, The gut microbiota of a patient with resistant tuberculosis is more comprehensively studied by culturomics than by metagenomics. *Eur. J. Clin. Microbiol. Infect. Dis.* 2013. **32**: 637–645.

32 **Dou, W., Zhang, J., Sun, A., Zhang, E., Ding, L., Mukherjee, S., Wei, X.** et al., Protective effect of naringenin against experimental colitis via suppression of Toll-like receptor 4/NF-kappaB signalling. *Br. J. Nutr.* 2013. **110**: 599–608.

33 **Cash, H. L., Whitham, C. V., Behrendt, C. L. and Hooper, L. V.**, Symbiotic bacteria direct expression of an intestinal bactericidal lectin. *Science* 2006. **313**: 1126–1130.

34 **Wang, L., Fouts, D. E., Starkel, P., Hartmann, P., Chen, P., Llorente, C., DePew, J.** et al., Intestinal REG3 lectins protect against alcoholic *Steatohepatitis* by reducing mucosa-associated microbiota and preventing bacterial translocation. *Cell Host Microbe* 2016. **19**: 227–239.

35 **Becattini, S., Taur, Y. and Pamer, E. G.**, Antibiotic-induced changes in the intestinal microbiota and disease. *Trends Mol. Med.* 2016. **22**: 458–478.

36 **Mutis, T., Cornelisse, Y. E. and Ottenhoff, T. H.**, Mycobacteria induce $CD4^+$ T cells that are cytotoxic and display Th1-like cytokine secretion profile: heterogeneity in cytotoxic activity and cytokine secretion levels. *Eur. J. Immunol.* 1993. **23**: 2189–2195.

37 **Flynn, J. L., Chan, J., Triebold, K. J., Dalton, D. K., Stewart, T. A. and Bloom, B. R.**, An essential role for interferon gamma in resistance to *Mycobacterium tuberculosis* infection. *J. Exp. Med.* 1993. **178**: 2249–2254.

38 **Van Crevel, R., Ottenhoff, T. H. and van der Meer, J. W.**, Innate immunity to *Mycobacterium tuberculosis*. *Clin. Microbiol. Rev.* 2002. **15**: 294–309.

39 **Kadowaki, N.**, Dendritic cells: a conductor of T cell differentiation. *Allergol. Int.* 2007. **56**: 193–199.

40 **Wu, H. J., Ivanov, II., Darce, J., Hattori, K., Shima, T., Umesaki, Y., Littman, D. R.** et al., Gut-residing segmented filamentous bacteria drive autoimmune arthritis via T helper 17 cells. *Immunity* 2010. **32**: 815–827.

41 **Nyarko-Adomfeh, C.**, Cardiac beta 2-adrenoceptors and the inotropic response to exercise in man. *Clin. Auton. Res.* 1991. **1**: 317–321.

42 **Negi, S., Das, D. K., Pahari, S., Nadeem, S. and Agrewala, J. N.**, Potential role of gut microbiota in induction and regulation of innate immune memory. *Front. Immunol.* 2019. **10**: 2441.

43 **Viaud, S., Daillere, R., Boneca, I. G., Lepage, P., Langella, P., Chamaillard, M., Pittet, M. J.** et al., Gut microbiome and anticancer immune response: really hot Sh*t! *Cell Death Differ.* 2015. **22**: 199–214.

44 **Cavalcanti, Y. V., Brelaz, M. C., Neves, J. K., Ferraz, J. C. and Pereira, V. R.**, Role of TNF-alpha, IFN-gamma, and IL-10 in the development of pulmonary tuberculosis. *Pulm. Med.* 2012. **2012**: 745483.

45 **Vlasova, A. N., Chattha, K. S., Kandasamy, S., Liu, Z., Esseili, M., Shao, L., Rajashekara, G.** et al., *Lactobacilli* and *bifidobacteria* promote immune homeostasis by modulating innate immune responses to human rotavirus in neonatal gnotobiotic pigs. *PLoS One* 2013. **8**: e76962.

46 **Matsusaki, T., Takeda, S., Takeshita, M., Arima, Y., Tsend-Ayush, C., Oyunsuren, T., Sugita, C., Yoshida, H.** et al., Augmentation of T helper type 1 immune response through intestinal immunity in murine cutaneous herpes simplex virus type 1 infection by probiotic *Lactobacillus plantarum* strain 06CC2. *Int. Immunopharm.* 2016. **39**: 320–327.

47 **Kato, I., Tanaka, K. and Yokokura, T.**, Lactic acid bacterium potently induces the production of interleukin-12 and interferon-gamma by mouse splenocytes. *Int. J. Immunopharmacol.* 1999. **21**: 121–131.

48 **Santos, K., Lukka, P. B., Grzegorzewicz, A., Jackson, M., Trivedi, A., Pavan, F., Chorilli, M.** et al., Primary lung dendritic cell cultures to assess efficacy of spectinamide-1599 against intracellular *Mycobacterium tuberculosis*. *Front. Microbiol.* 2018.**9**: 1895.

49 **Wolf, A. J., Linas, B., Trevejo-Nunez, G. J., Kincaid, E., Tamura, T., Takatsu, K. and Ernst, J. D.**, *Mycobacterium tuberculosis* infects dendritic cells with high frequency and impairs their function in vivo. *J. Immunol.* 2007. **179**: 2509–2519.

50 **Cooper, A. M. and Khader, S. A.**, The role of cytokines in the initiation, expansion, and control of cellular immunity to tuberculosis. *Immunol. Rev.* 2008. **226**: 191–204.

51 **Flynn, J. L., Goldstein, M. M., Chan, J., Triebold, K. J., Pfeffer, K., Lowenstein, C. J., Schreiber, R.** et al., Tumor necrosis factor-alpha is required in the protective immune response against *Mycobacterium tuberculosis* in mice. *Immunity* 1995. **2**: 561–572.

52 **Domingo-Gonzalez, R., Prince, O., Cooper, A. and Khader, S. A.**, Cytokines and chemokines in *Mycobacterium tuberculosis* infection. *Microbiol. Spectr.* 2016.**4**. https//doi.org/10.1128/microbiolspec.TBTB2-0018-2016.

53 **Kwon, O. J.**, The role of nitric oxide in the immune response of tuberculosis. *J. Korean Med. Sci.* 1997. **12**: 481–487.

54 **Pahari, S., Negi, S., Aqdas, M., Arnett, E., Schlesinger, L. S. and Agrewala, J. N.**, Induction of autophagy through CLEC4E in combination with TLR4: an innovative strategy to restrict the survival of *Mycobacterium tuberculosis*. *Autophagy* 2020. **16**: 1021–1043.

55 **Khan, N., Pahari, S., Vidyarthi, A., Aqdas, M. and Agrewala, J. N.**, Stimulation through CD40 and TLR-4 is an effective host directed therapy against *Mycobacterium tuberculosis*. *Front Immunol.* 2016. **7**: 386.

56 **Pahari, S., Kaur, G., Negi, S., Aqdas, M., Das, D. K., Bashir, H., Singh, S.** et al., Reinforcing the functionality of mononuclear phagocyte system to control tuberculosis. *Front. Immunol.* 2018. **9**: 193.

57 **Pahari, S.**, **Kaur, G.**, **Aqdas, M.**, **Negi, S.**, **Chatterjee, D.**, **Bashir, H.**, **Singh, S.** et al., Bolstering immunity through pattern recognition receptors: a unique approach to control tuberculosis. *Front. Immunol.* 2017. **8**: 906.

58 **Negi, S.**, **Pahari, S.**, **Das, D. K.**, **Khan, N. and Agrewala, J. N.**, Curdlan limits *Mycobacterium tuberculosis* survival through STAT-1 regulated nitric oxide production. *Front. Microbiol.* 2019. **10**: 1173.

59 **Pahari, S.**, **Khan, N.**, **Aqdas, M.**, **Negi, S.**, **Kaur, J. and Agrewala, J. N.**, Infergen stimulated macrophages restrict *Mycobacterium tuberculosis* growth by autophagy and release of nitric oxide. *Sci. Rep.* 2016. **6**: 39492.

60 **Hartman, A. L.**, **Lough, D. M.**, **Barupal, D. K.**, **Fiehn, O.**, **Fishbein, T.**, **Zasloff, M. and Eisen, J. A.**, Human gut microbiome adopts an alternative state following small bowel transplantation. *Proc. Natl. Acad. Sci. USA* 2009. **106**: 17187–17192.

61 **Kabeerdoss, J.**, **Sankaran, V.**, **Pugazhendhi, S. and Ramakrishna, B. S.**, *Clostridium leptum* group bacteria abundance and diversity in the fecal microbiota of patients with inflammatory bowel disease: a case-control study in India. *BMC Gastroenterol.* 2013. **13**: 20.

62 **Layton, A.**, **McKay, L.**, **Williams, D.**, **Garrett, V.**, **Gentry, R. and Sayler, G.**, Development of bacteroides 16S rRNA gene TaqMan-based real-time PCR assays for estimation of total, human, and bovine fecal pollution in water. *Appl. Environ. Microbiol.* 2006. **72**: 4214–4224.

63 **Tuomisto, S.**, **Karhunen, P. J. and Pessi, T.**, Time-dependent post mortem changes in the composition of intestinal bacteria using real-time quantitative PCR. *Gut Pathog.* 2013. **5**: 35.

64 **Rinttila, T.**, **Kassinen, A.**, **Malinen, E.**, **Krogius, L. and Palva, A.**, Development of an extensive set of 16S rDNA-targeted primers for quantification of pathogenic and indigenous bacteria in faecal samples by real-time PCR. *J. Appl. Microbiol.* 2004. **97**: 1166–1177.

65 **Bacchetti De Gregoris, T.**, **Aldred, N.**, **Clare, A. S. and Burgess, J. G.**, Improvement of phylum- and class-specific primers for real-time PCR quantification of bacterial taxa. *J. Microbiol. Methods* 2011. **86**: 351–356.

66 **Cossarizza, A.**, **Chang, H. D.**, **Radbruch, A.**, **Acs, A.**, **Adam, D.**, **Adam-Klages, S.**, **Agace, W. W.** et al., Guidelines for the use of flow cytometry and cell sorting in immunological studies (second edition). *Eur. J. Immunol.* 2019. **49**: 1457–1973.

Abbreviations: **Abx**: antibiotics · **BCG**: Bacillus Calmette-Guerin · **DOTS**: Directly Observed Treatment Short-course · **INH**: isonicotinylhydrazide · **TB**: tuberculosis · ***Mtb***: *Mycobacterium tuberculosis* · **CD**: cluster of differentiation · **NOD**: nucleotide oligomerization domain · **PPD**: purified protein derivative · **CFSE**: carboxyfluoresceinsuccinimidyl ester · **PRRs**: pattern recognition receptors · **PD-L**: programmed cell death ligand · **RegIIIγ**: regenerating islet-derived protein 3 gamma

Full correspondence: Prof. Javed N. Agrewala, Immunology Division, CSIR-Institute of Microbial Technology, Chandigarh, India.
e-mail: jagrewala@iitrpr.ac.in

The peer review history for this article is available at https://publons.com/publon/10.1002/eji.202048556

Received: 18/1/2020
Revised: 5/7/2020
Accepted: 14/7/2020
Accepted article online: 16/7/2020